J Comput Neurosci
DOI 10.1007/s10827-007-0032-z

Intrinsic bursting enhances the robustness of a neural network model of sequence generation by avian brain area HVC

Dezhe Z. Jin · Fethi M. Ramazanoğlu · H. Sebastian Seung

Received: 25 September 2006 / Revised: 9 February 2007 / Accepted: 13 March 2007

Abstract Avian brain area HVC is known to be important for the production of birdsong. In zebra finches, each RA-projecting neuron in HVC emits a single burst of spikes during a song motif. The population of neurons is activated in a precisely timed, stereotyped sequence. We propose a model of these burst sequences that relies on two hypotheses. First, we hypothesize that the sequential *order* of bursting is reflected in the excitatory synaptic connections between neurons. Second, we propose that the neurons are intrinsically bursting, so that burst *duration* is set by cellular properties. Our model generates burst sequences similar to those observed in HVC. If intrinsic bursting is removed from the model, burst sequences can also be produced. However, they require more fine-tuning of synaptic strengths, and are therefore less robust. In our model, intrinsic bursting is caused by dendritic calcium spikes, and strong spike frequency adaptation in the soma contributes to burst termination.

Keywords Songbird · Associative chaining model · Dendritic spike · Sequence generation · Computational model

Action Editor: Alain Destexhe

D. Z. Jin (✉)
Department of Physics,
The Pennsylvania State University,
104 Davey Lab, University Park, PA 16802, USA
e-mail: djin@phys.psu.edu

F. M. Ramazanoğlu
Department of Physics,
Massachusetts Institute of Technology,
Cambridge, MA 02139, USA

H. S. Seung
Howard Hughes Medical Institute
and Department of Brain and Cognitive Sciences,
Massachusetts Institute of Technology,
Cambridge, MA 02139, USA

1 Introduction

How does the brain generate behaviors that are composed of long sequences of actions, such as language and musical performance? According to one idea, sequential behaviors are generated by the sequential activation of groups of neurons. In the associative chaining model, the neurons of one group directly excite the neurons of the next group, so that sequential order is directly embedded in the structure of excitatory synaptic connectivity. This model was criticized by Lashley on theoretical grounds as insufficient for explaining the full complexity of sequential behaviors (Lashley 1951). However, the model has never actually been tested through neurobiological experiments.

Recent progress in the neurobiology of birdsong has set the stage for testing the associative chaining model in a non-human animal (Chi and Margoliash 2001; Doupe and Kuhl 1999; Fee et al. 2004; Hahnloser et al. 2002; Konishi 1965; Leonardo and Fee 2005; Nottebohm et al. 1976; Williams 2004; Yu and Margoliash 1996). The goal of this paper is to give a biophysically realistic implementation of the associative chaining model applied to birdsong. As will be seen later, our implementation of the model leads to a number of predictions that can be tested experimentally.

The zebra finch sings a single, highly stereotyped song that consists of repetitions of a motif, typically 0.5–1 s in

duration (Immelmann 1969).[1] The motif is composed of 3–7 smaller vocal gestures called song syllables. Lesion studies indicate that avian brain area HVC (used as a proper name) plays an important role in the production of birdsong (Nottebohm et al. 1976). Of the several classes of neurons found in HVC (Dutar et al. 1998; Fortune and Margoliash 1995; Katz and Gurney 1981; Kubota and Taniguchi 1998; Lewicki 1996; Mooney 2000; Nixdorf et al. 1989; Wild et al. 2005), those that project to RA (robust nucleus of the arcopallium) are of prime importance for song production, because RA drives the motor neurons that control vocalization (Nottebohm et al. 1976, 1982; Vicario 1991) (Fig. 1(a)). We will refer to this class of HVC neurons as RA-projecting, HVC(RA) neurons for short.

In zebra finches, an HVC(RA) neuron emits exactly one burst of several spikes during a song motif[2] (Fee et al. 2004; Hahnloser et al. 2002) (Fig. 1(b)). The timing of the burst is remarkably precise, with a jitter of less than a millisecond relative to the song. The burst onset times of the neurons are thought to be distributed throughout the motif. This means that the population of HVC(RA) neurons generate a highly stereotyped, precisely timed sequence of bursts. This burst sequence drives activity in RA, which in turn drives the motor neurons that control vocalization (Fee et al. 2004; Hahnloser et al. 2002; Leonardo and Fee 2005).

In this paper, we will assume that the burst sequences are generated within HVC itself, rather than driven by input from an upstream brain area. While this assumption is not yet proven, it is consistent with existing experimental data. Upstream nuclei such as NIf (nucleus interfacialis of the nidopallium) and Uva (nucleus uvaeformis) project to HVC (Nottehbohm et al. 1976, 1982). However, lesion studies show that NIf is not necessary for song (Cardin et al. 2004). While Uva is necessary for song (Coleman and Vu 2005), there is no evidence yet that activity of Uva neurons is precisely timed enough to drive burst sequences in HVC. Therefore it seems reasonable to assume, at least provisionally, that the burst sequences are actually generated in HVC itself.

What circuit and cellular mechanisms in HVC could be responsible for burst sequences? We will advance two hypotheses.

Hypothesis 1 *If neurons A and B are activated consecutively in the burst sequence, then there is likely to be an excitatory synapse from A to B.*

[1]Note that the associative chaining model is ideally suited to the stereotypy of zebra finch song, which contrasts with the extreme diversity of sequences generated by humans. Lashley argued that a hierarchical neural representation is necessary for generating such diversity (Lashley 1951).

[2]To be more accurate, about half the HVC(RA) neurons do this, while the other half are inactive (Hahnloser et al. 2002).

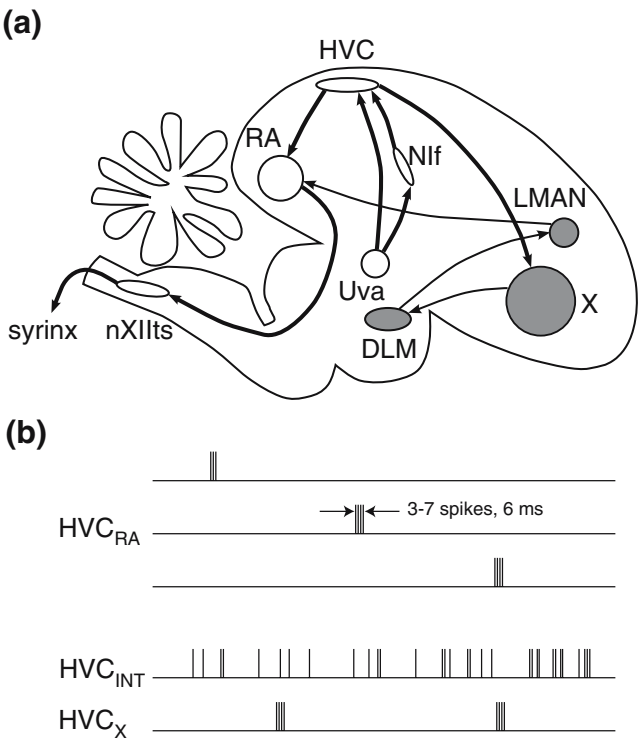

Fig. 1 Avian brain area HVC. (**a**) HVC projects to RA and X. RA drives motor neurons that control song production. X is the beginning of the anterior forebrain pathway, which is important for song learning but not production of previously learned song. (**b**) Activity of HVC neurons. During a song motif, HVC(RA) neurons generate a single burst of spikes, HVC(X) neurons generate several bursts, and HVC(I) neurons are active throughout

Hypothesis 2 *HVC(RA) neurons are intrinsically bursting, so that burst duration is set by cellular properties.*

The first hypothesis follows the classic associative chaining model of sequence generation. According to the hypothesis, structure is related to function: the sequential *order* of bursting is embedded in the organization of excitatory synapses between HVC(RA) neurons. The second hypothesis relates the abstract associative chaining model to specific biophysical mechanisms.

In the following, we first briefly overview our main results. We then summarize the known facts about HVC, and argue that a reduced model containing only HVC(RA) neurons is appropriate for explaining burst sequences in HVC. Finally, we discuss the possible synaptic connectivity between HVC(RA) neurons. We focus on a particular realization of Hypothesis 1, in which the HVC(RA) neurons are divided into groups, and the groups are ordered in a sequence. Each group makes excitatory synapses onto the next group. If group 1 is activated by external input, then it activates group 2, which activates group 3, and so on. Because the groups are completely disjoint, a single neuron is activated only once during the whole sequence. Abeles has

utilized this synaptic connectivity in his synfire chain model, which stresses synchronous spiking of neurons in each group (Abeles 1982, 1991). Others have utilized this connectivity in neural network models based on firing rates[3] (Amari 1972; Kleinfeld 1986; Sompolinsky and Kanter 1986).

1.1 Overview

In the Results, we first study an associative chaining model without intrinsic bursting in HVC(RA) neurons. We show that the model can generate burst sequences like those seen in HVC. However, there is a problem: the model requires fine-tuning of synaptic strengths. Since the response of a neuron depends on the amplitude and duration of synaptic input, the number of spikes in a burst depends strongly on synaptic strengths. If synapses are too strong, then there is runaway activity, in which successive neurons in the sequence produce longer and longer bursts of spikes. If synapses are too weak, then the activity decays to zero.

To solve this robustness problem, we utilize Hypothesis 2, which is that HVC(RA) neurons are equipped with intrinsic cellular mechanisms for generating bursts. When a burst of spikes is initiated, it is a stereotyped event, with only a weak dependence on the amplitude or duration of synaptic input. As a result, little tuning of synaptic strengths is required to produce burst sequences. This improved robustness is demonstrated with numerical simulations of our model.

Our Hypothesis 2 is not the only way of solving the robustness problem, but it is arguably the simplest. Obviously it is easier to construct a neural circuit that generates bursts, if the elements in the circuit produce bursts intrinsically. Other ways of solving the robustness problem are mentioned in Section 4.

Whether HVC(RA) neurons indeed possess intrinsic bursting mechanisms is currently unknown. A number of such mechanisms have been studied in other neurons (Brumberg et al. 2000; Franceschetti et al. 1995; Mattia et al. 1997; Schwindt and Crill 1999; Traub et al. 1994; Wong and Stewart 1992), and any of them would be sufficient for generating the bursts observed in HVC. We can only speculate as to the mechanisms that could be involved. In our model, the dendrites of HVC(RA) neurons produce a calcium spike, due to the presence of voltage-activated calcium channels. This calcium spike depolarizes the soma, producing a burst of sodium spikes.

Calcium spikes can last tens of milliseconds in hippocampal and cortical neurons (Golding et al. 1999; Schwindt and Crill 1999; Wei et al. 2001). If HVC(RA) neurons have calcium spikes of similar duration, what could account for the fact that bursts in HVC have an average duration of 6 ms (Hahnloser et al. 2002)? To limit the duration of sodium spiking, our model incorporates a biophysical property that has been observed in HVC(RA) neurons in vitro, strong spike frequency adaptation (Dutar et al. 1998; Mooney and Prather 2005; Wild et al. 2005). As discussed in Section 3, this causes sodium spiking to terminate before the end of the calcium spike. One could also imagine that HVC neurons possess calcium spikes that last for just 6 ms, in which case strong spike frequency adaptation in the soma would be less crucial.

The burst duration in our model is determined by intrinsic cellular properties, rather than circuit properties. Therefore it is natural to ask whether fine-tuning of intrinsic cellular properties is required to generate bursting. We show that this is not the case, as the number of spikes per burst is not very sensitive to parameters of our model neuron.

Before proceeding further, we should say a few words about our methodology, which could be described as "top-down." Table 1 lists four levels of description of HVC. We begin near the top, with burst sequences. In order to explain them, we make Hypothesis 1 about correlational connectivity and Hypothesis 2 about intrinsic bursting. Hypothesis 2 is further elaborated by adding strong spike frequency adaptation. Our model shows how these hypothetical neuron and network properties could help generate burst sequences, and therefore demonstrates their potential functional significance for birdsong. Moving further down in the table, specific channels are proposed as biophysical mechanisms for the hypothetical single neuron properties. These proposals are useful, because they suggest specific ways of testing the neuron-level hypotheses experimentally (see Section 4). However, the primary subject of this paper is the functional implications of intrinsic cellular properties for sequence generation, rather than the detailed biophysical mechanisms of these intrinsic properties.

We have pursued a top-down modeling approach, because the bottom-up approach is not possible at this time. The channel properties of HVC neurons cannot serve as a starting point for modeling, because so little is known about them. A top-down approach has the advantage that it guides research by focusing attention on neuron and

Table 1 HVC model and levels of description

Behavior	Song
Network	Burst sequences
	Correlational connectivity
Neuron	Intrinsic bursting
	Strong spike frequency adaptation
Channel	Dendrite: I_{Ca}, I_{CaK}
	Soma: I_{KLT}, I_{KHT}

[3] In the more general correlation matrix model studied by these authors, a single neuron is allowed to belong to more than one group.

channel properties that are most significant for behavioral function.

1.2 Synaptic organization of HVC

In this section, we summarize the current knowledge about synaptic connectivity of HVC, and introduce a reduced model for sequence generation that focuses on the excitatory synapses between HVC(RA) neurons, and omits the other classes of neurons in HVC.

HVC contains two classes of projection neurons, those that project to RA (HVC(RA)), and those that project to area X (HVC(X)); it also contains interneurons (HVC(I)) (Dutar et al. 1998; Fortune and Margoliash 1995; Katz and Gurney 1981; Kubota and Taniguchi 1998; Lewicki 1996; Mooney 2000; Nixdorf et al. 1989; Wild et al. 2005). The projection to RA is important for song production, as RA drives motor neurons that control vocalization (Nottebohm et al. 1976, 1982; Vicario 1991). The projection to X enters the anterior forebrain pathway, which is important for song learning but not necessary for song production (Brainard and Doupe 2000).

Figure 2(a) is our best guess about the synaptic connectivity of HVC, given the limited information that exists in the literature (Mooney and Prather 2005). According to the figure, HVC(RA) neurons make excitatory synapses onto both HVC(RA) and HVC(X) neurons. In contrast, HVC(X) neurons make no excitatory synapses onto other projection neurons. Both types of projection neurons make excitatory synapses on interneurons, and receive inhibitory synapses from them.[4] In the following, we assume that the diagram of Fig. 2(a) is correct, and argue that the simplified versions shown in Fig. 2(b and c) should be good approximations.

Interneurons are much less temporally selective than projection neurons in their song-related activity (Fig. 1(b)). During a song motif, HVC(RA) neurons fire a single burst of spikes (Hahnloser et al. 2002), and HVC(X) neurons fire a few bursts (Kozhevnikov and Fee 2006). In contrast, HVC(I) neurons fire at many times during a song motif (Hahnloser et al. 2002).

If we make the approximation that interneurons have constant firing rates during song, their dynamic inhibitory input to the projection neurons can be replaced by a static conductance. With this approximation, we can omit the interneurons from Fig. 2(a), which yields the reduced model shown in Fig. 2(b).

Neglecting synaptic inhibition may seem like a drastic step. However, it seems justified provided that the goal of modeling is to explain sequence generation. Since inhibition lacks temporal selectivity, its main role is likely to be regulation of the overall level of activity in projection neurons, which might enhance the robustness of sequence generation.

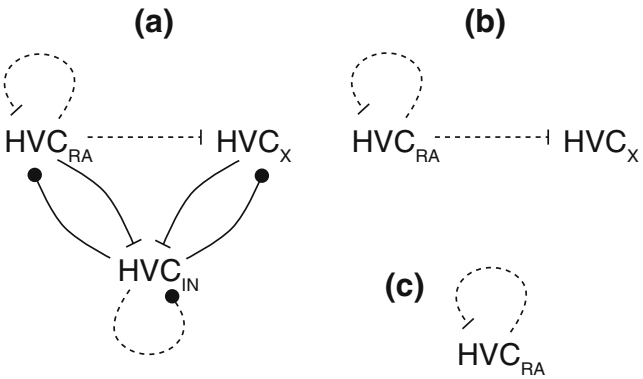

Fig. 2 Synaptic organization of HVC and reduced models. (**a**) Hypothesized synaptic organization of HVC. HVC(RA) neurons excite each other and HVC(X) neurons. Both HVC(RA) and HVC(X) neurons excite HVC(I) neurons, and receive inhibition from them. The evidence for recurrent inhibition (*solid lines*) is strong (Mooney and Prather 2005). The excitatory interactions between projection neurons (*dashed lines*) are more speculative. The lack of synapses from HVC(X) to HVC(RA) neurons is based on Scharff et al. (2000). (**b**) Reduced model with projection neurons only. If the HVC(I) neurons have firing rates that are approximately constant in time, then they can be omitted, leaving a reduced model consisting of projection neurons only. (**c**) Further reduced model with HVC(RA) neurons only. Since there are essentially no backprojections from HVC(X) neurons to HVC(RA) neurons, one can consider a reduced model consisting of HVC(RA) neurons only

In the reduced model of Fig. 2(b), HVC(RA) neurons send feedforward drive to HVC(X) neurons, but receive no signals from them, which implies that HVC(X) neurons are irrelevant to the dynamics of HVC(RA) neurons. Therefore we omit the HVC(X) neurons, as the projection to area X is not necessary for song production anyway (Brainard and Doupe 2000). This leads to a reduced model containing only HVC(RA) neurons, as shown in Fig. 2(c). Note that this reduction depends on the assumption that there are no synapses from HVC(X) neurons to HVC(RA) neurons, as in Fig. 2(a). This is consistent with the fact that targeted destruction of HVC(X) neurons does not cause deterioration of song in adult zebra finches (Scharff et al. 2000).

1.3 Correlational models of synaptic connectivity

In the preceding section, we argued that a reduced model of HVC containing only HVC(RA) neurons is a good starting point for understanding sequence generation. But the synaptic connectivity between HVC(RA) neurons is largely unknown. In the Introduction, we proposed Hypothesis 1: if neurons A and B are activated consecutively in the burst sequence, then there is likely to be an excitatory synapse

[4]This diagram is based primarily on the work of Mooney and Prather (2005). The evidence for recurrent inhibition is strong, but the excitatory interactions between projection neurons are somewhat speculative.

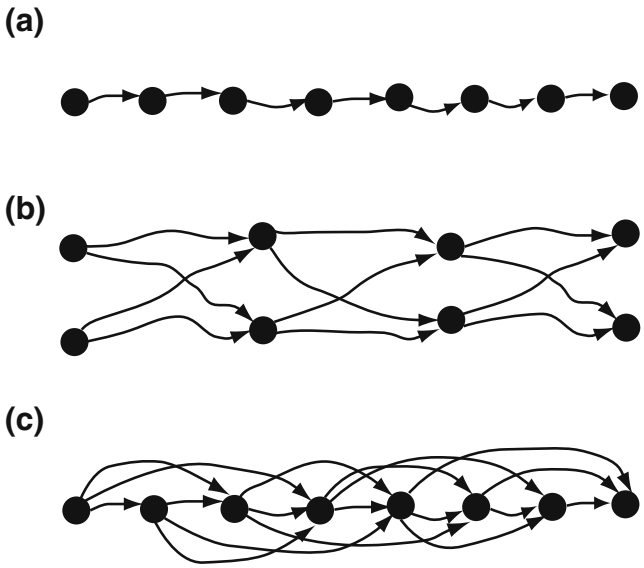

Fig. 3 Some synaptic connectivities suitable for sequence generation. The connectivity of a neural network can be represented as a directed graph. (**a**) A unidirectional chain of neurons. (**b**) A unidirectional chain of groups. (**c**) A more general correlational model

from A to B. In other words, if neuron A fires just before neuron B, we can infer that A probably helped *cause* B to fire by giving it direct excitatory synaptic input. The inference is probabilistic, since some imprecision of wiring is expected in a neurobiological system. Since we are inferring causation from temporal correlation, Hypothesis 1 can be called a correlational model of connectivity.

To make the implications of the correlational model more explicit, it is worth stating the conditions under which an excitatory synapse is *not* expected between neurons A and B. If neuron A fires long before neuron B, there should be no synapse between them (temporal contiguity is important). If neuron A fires *after* neuron B, there should be no synapse from A to B (temporal order is important).[5]

Many correlational models of synaptic connectivity have been proposed for sequence generation (Abeles 1982; Amari 1972; Kleinfeld 1986; Sompolinsky and Kanter 1986). The simplest is a unidirectional chain of neurons (Fig. 3(a)). Each neuron makes an excitatory synapse onto the next neuron in the chain. Somewhat more complex is a unidirectional chain of groups of neurons. Each group makes excitatory synapses onto the next group (Fig. 3(b)). Another possibility is that each neuron makes synapses onto several of its successors in the sequence (Fig. 3(c)), which is not a simple chain architecture.[6]

[5]While these statements are applicable for an idealized model of sequence generation, a real neurobiological system might deviate somewhat from the ideal, as detailed in Section 4.

[6]Figure 3(c) is actually the most general of the models, as both Fig. 3(a and b) can be generated from it by deleting connections.

In the rest of the paper, we will study the model of Fig. 3(b), the unidirectional chain of groups. Our numerical simulations will have 200 groups, each containing 30 neurons, for a total of 6,000 neurons. This model should be regarded as just one possible implementation of the correlational idea proposed in Hypothesis 1. But our findings about the role of intrinsic bursting in generating sequences are expected to apply to other correlational connectivity, such as the one in Fig. 3(c).

2 Materials and methods

2.1 Two-compartment model of HVC(RA) neuron

Currently, there are no experimental data on ion channel properties in HVC(RA) neurons. We therefore construct a minimal conductance-based model of HVC(RA) neurons following three guidelines: (1) The model must be biophysically plausible; (2) the model must reproduce known properties of HVC(RA) neurons, which mainly come from experiments that injected currents to soma (Dutar et al. 1998; Kubota and Taniguchi 1998; Mooney et al. 2001; Wild et al. 2005); (3) the model must exhibit robust burst spike propagation through excitatory connections between neurons.

The minimal model consists of somatic and dendritic compartments. It is based on previous two-compartment models of cortical neurons (Crook et al. 1998; Pinsky and Rinzel 1994; Wang 1999). The somatic compartment contains Hudgkin–Huxley type sodium and delayed rectifying potassium conductances for spike generation (Hodgkin and Huxley 1952), as well as a leak conductance. In addition, we introduce both high-threshold and low-threshold potassium conductances. The high-threshold potassium (KHT) conductance is activated at high membrane potentials, and provides re-polarizing currents during the spiking. KHT conductance, as shown in rat hippocampal interneurons (Lien and Jonas 2003), auditory neurons in medial nucleus of the trapezoid body of mice (Wang et al. 1998), and auditory neurons in avian nucleus magnocellularis (Rathouz and Trussell 1998), enables the neuron to spike at high frequency. The low-threshold potassium (KLT) conductance is introduced to account for the strong spike-frequency adaptation observed in HVC(RA) neurons (Dutar et al. 1998; Mooney et al. 2001; Mooney and Prather 2005; Wild et al. 2005). KLT conductance has been shown to produce a similar spike frequency adaptation in a number of neuron types, including auditory neurons in avian nucleus magnocellularis (Rathouz and Trussell 1998; Reyes et al. 1994), bushy cells in ventral cochlear nucleus (Manis and Marx 1991), auditory neurons in the medial nucleus of the trapezoid body of rats (Dodson et al. 2002) and mice (Wang

et al. 1998), and auditory neurons in the gerbil medial superior olive (Svirskis et al. 2002). KLT conductance is activated at subthreshold membrane potentials.

The dendritic compartment contains a leak conductance, a high-threshold calcium conductance, and a calcium-activated potassium conductance. The calcium and potassium conductance enable a calcium spike in the dendrite if depolarized over the threshold, as observed in dendrites of many types of neurons, such as mammalian hippocampal and cortical neurons, as well as cerebellar Purkinje neurons (Golding et al. 1999; Hausser et al. 2000). Biophysical plausibility of our model is ensured since the conductances are taken from previous experimental data in other types of neurons. In the man text, we have shown that this minimal model also satisfies the other two guidelines.

The membrane potentials V_s and V_d of soma and dendrite obey the following dynamical equations:

$$C_m A_s \frac{dV_s}{dt} = A_s(I_{Ls} + I_{Na} + I_K + I_{KHT} + I_{KLT} + I_{FFs}) + I_{ext} + (V_d - V_s)/R_c,$$

$$C_m A_d \frac{dV_d}{dt} = A_d\left(I_{Ld} + I_{Ca} + I_{CaK} + I_{syn} + I_{FFd}\right) + (V_s - V_d)/R_c.$$

Here C_m=1 μF/cm^2 is the membrane capacitance, A_s=100 μm^2 and A_d=50,000 μm^2 are the surface areas of the soma and the dendrite, respectively. For the soma, I_{Ls}=$g_{Ls}(E_r-V_s)$ is the leak current, with conductance g_{Ls}=0.05 mS/cm^2 and reversal potential E_r=−85 mV; I_{Na}=$g_{Na}m^3\times h(E_{Na}-V_s)$ is the sodium current, with conductance g_{Na}=100 mS/cm^2, reversal potential E_{Na}=55 mV, and gating variables m and h; I_K=$g_K n^4(E_K-V_s)$ is the potassium current, with conductance g_K=2 mS/cm^2, reversal potential E_K=−90 mV, and gating variable n; I_{KHT}=$g_{KHT}w(E_K-V_s)$ is the high threshold potassium current, with conductance g_{KHT}=300 mS/cm^2 and gating variable w. I_{KLT}=$g_{KLT}l(E_K-V_s)$ is the low threshold potassium current, with conductance g_{KLT}=25 mS/cm^2 and gating variable l; I_{FFs}=$-g_{FFs}V_s$ is the feedforward excitatory input to the soma, with a constant conductance g_{FFs}; I_{ext} is the external current injection to soma; R_c=250 MΩ is the resistance of the connection between soma and dendrite. For the dendrite, I_{Ld}=$g_{Ld}(E_r-V_d)$ is the leak current with g_{Ld}=0.1 mS/cm^2; I_{Ca} = $g_{Ca}m_\infty^2(E_{Ca}-V_d)$ is the high threshold calcium current with conductance g_{Ca}=200 mS/cm^2, reversal potential E_{Ca}=120 mV, and voltage dependent factor m_∞=1/(1+exp(−(V_d−20)/15)); I_{CaK}=$g_{CaK}q(E_K-V_d)$ is the calcium dependent potassium current, with conductance g_{CaK}=100 mS/cm^2, and calcium dependent variable q; I_{syn}=$-g_{syn}V_d$ is the excitatory synaptic current. Calcium concentration follows a first order kinetics d[Ca^{2+}]/dt=0.1I_{Ca}−[Ca^{2+}]/τ_{Ca}, with the decay time constant τ_{Ca}=100 ms. I_{FFd}=$-g_{FFd}V_d$ is the feedforward excitatory to the dendrite, with a constant conductance g_{FFd}; The synaptic conductance follows a "kick-and-decay" kinetics: $g_{syn}\rightarrow g_{syn}+G$ when a spike arrives from another HVC(RA) neuron at a synapse with conductance G, and dg_{syn}/dt=$-g_{syn}/\tau_{syn}$ in between spikes with synaptic time constant τ_{syn}=5 ms.

The general equation for the gating variables m, h, n is

$$\frac{dx}{dt} = \alpha_x(V)(1-x) - \beta_x(V)x,$$

where x=m, h, n. The voltage dependent coefficients of the gating variables are:

$$\alpha_m = -0.5(V+22)/(\exp(-(V+22)/10)-1),$$
$$\beta_m = 20\ \exp(-(V+47)/18);$$
$$\alpha_h = 0.35\ \exp(-(V+34)/20),$$
$$\beta_h = 5/(\exp(-(V+4)/10)+1);$$
$$\alpha_n = -0.075(V+30)/(\exp(-(V+30)/10)-1),$$
$$\beta_n = 0.1\ \exp(-(V+40)/80).$$

The general equation for the gating variables x=w, l, q is

$$\frac{dx}{dt} = (x_\infty(V) - x)/\tau_x.$$

Here, $w_\infty(V)$ = 1/(exp(−V/5)+1), τ_w = 1 ms; l_∞=1/(exp(−(V+40)/5)+1), τ_l = 10 ms; and q_∞([Ca^{2+}])=(0.0005[Ca^{2+}])^2, τ_q([Ca^{2+}])=(0.0338)/(min(0.0001[Ca^{2+}], 0.01)+0.001). The kinetics of the gating variable q of the calcium dependent potassium conductance is taken from Crook et al. (1998).

The properties of the model neuron under current injection to the soma are illustrated in Fig. 4, which shows that the KLT conductance in the soma produces a strong spike frequency adaptation as observed in the experiments (Dutar et al. 1998; Mooney et al. 2001; Wild et al. 2005). The key properties of the KLT conductance are that it is large when the membrane potential is large and that it does not inactivate. Figure 4(a) shows traces of subthreshold somatic membrane potentials under step current injections. For the largest inject current in the figure, a brief subthreshold overshoot of the membrane potential can be seen. This is because the activation of the KLT conductance is slower than the rise of the membrane potential when the magnitude of the step current is large. Activation of the KLT conductance is also responsible for a sublinear dependence of the equilibrium membrane potential on the applied current, as shown in Fig. 4(b). The slow activation of the KLT conductance permits a time window for producing a few transient spikes with suprathreshold step currents, as shown in Fig. 4(c). In this case, as the KLT conductance becomes fully activated, the membrane poten-

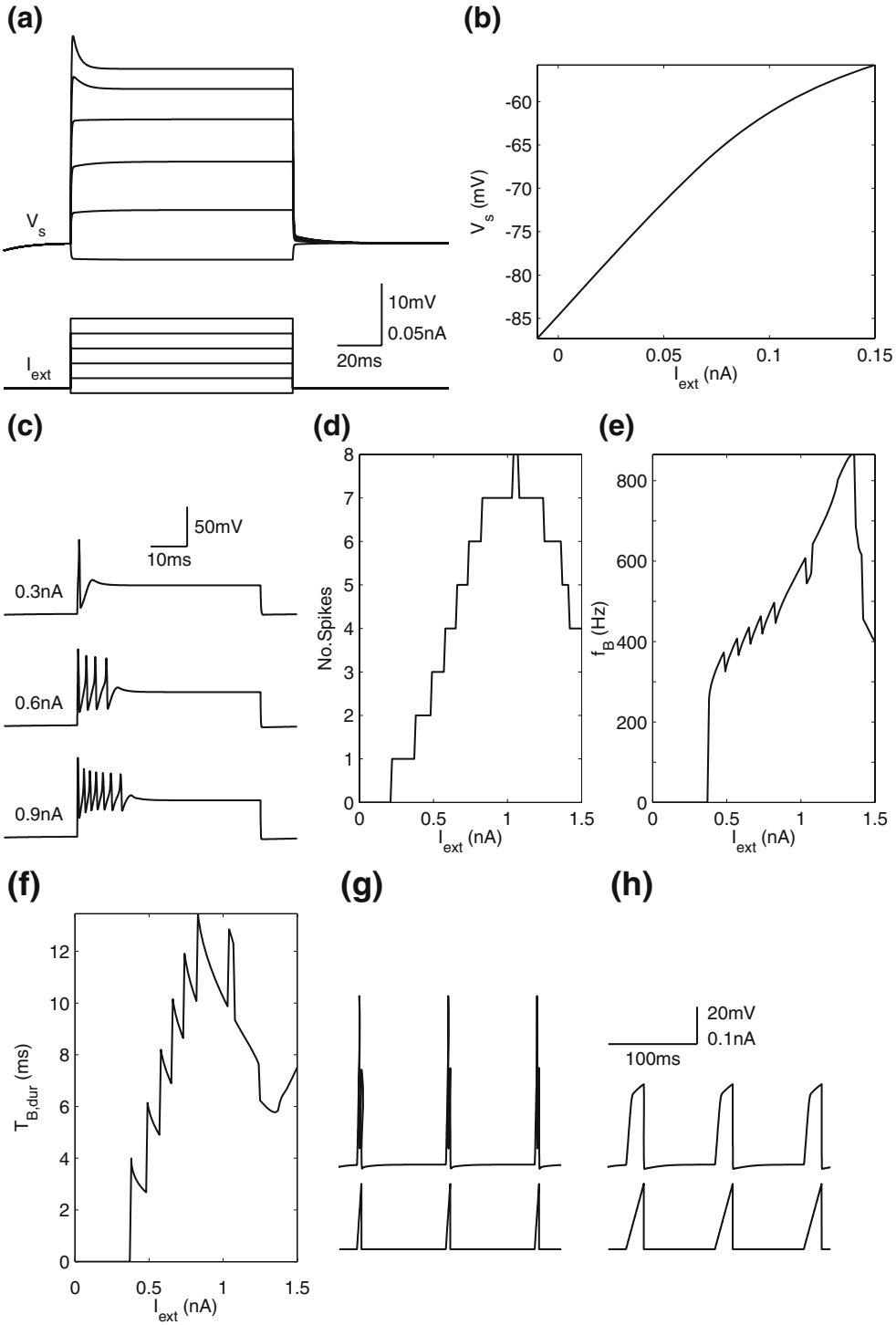

Fig. 4 Strong spike frequency adaptation of the two-compartment HVC(RA) neuron shown with somatic membrane potential responses under current injections to soma. (**a**) Traces of subthreshold membrane potentials under step current injection of 100 ms duration. (**b**) The equilibrium value of the subthreshold membrane potential as a function of the inject current. (**c**) Traces of supra-threshold membrane potentials under step current injection of 50 ms. The number of spikes is limited by activation of the KLT current. (**d**) Number of spikes as a function of the inject step current of 50 ms duration. (**e**) Instantaneous spike frequency in the condition of D. (**f**) Durations of the spiking activity in the condition of D. (**g**) Repeated spiking of the neuron under 10 Hz triangular current pulses. The width and the peak of the pulse are 5 ms and 0.5 nA, respectively. (**h**) When the ramp-up in the triangular pulse is slow (here at 20 ms), the KLT current can prevent the neuron from spiking

tial settles to an equilibrium plateau, and further spiking is suppressed due to the large KLT conductance. The number of transient spikes initially increases in steps with the increasing inject current up to a maximum at about 8, then decreases at very large inject currents due to depolarization block (Fig. 4(d)). The neuron never spikes regularly at any inject current due to the KLT conductance. The high threshold potassium conductance helps the neuron to spike at high frequency before the full activation of the KLT conductance. When there is more than one spike, the instantaneous spike frequency is about 400–800 Hz (Fig. 4(e)), and the duration of the spike burst is on the order of 2–13 ms (Fig. 4(f)), reflecting the activation time scale of the KLT conductance (10 ms in the model). The

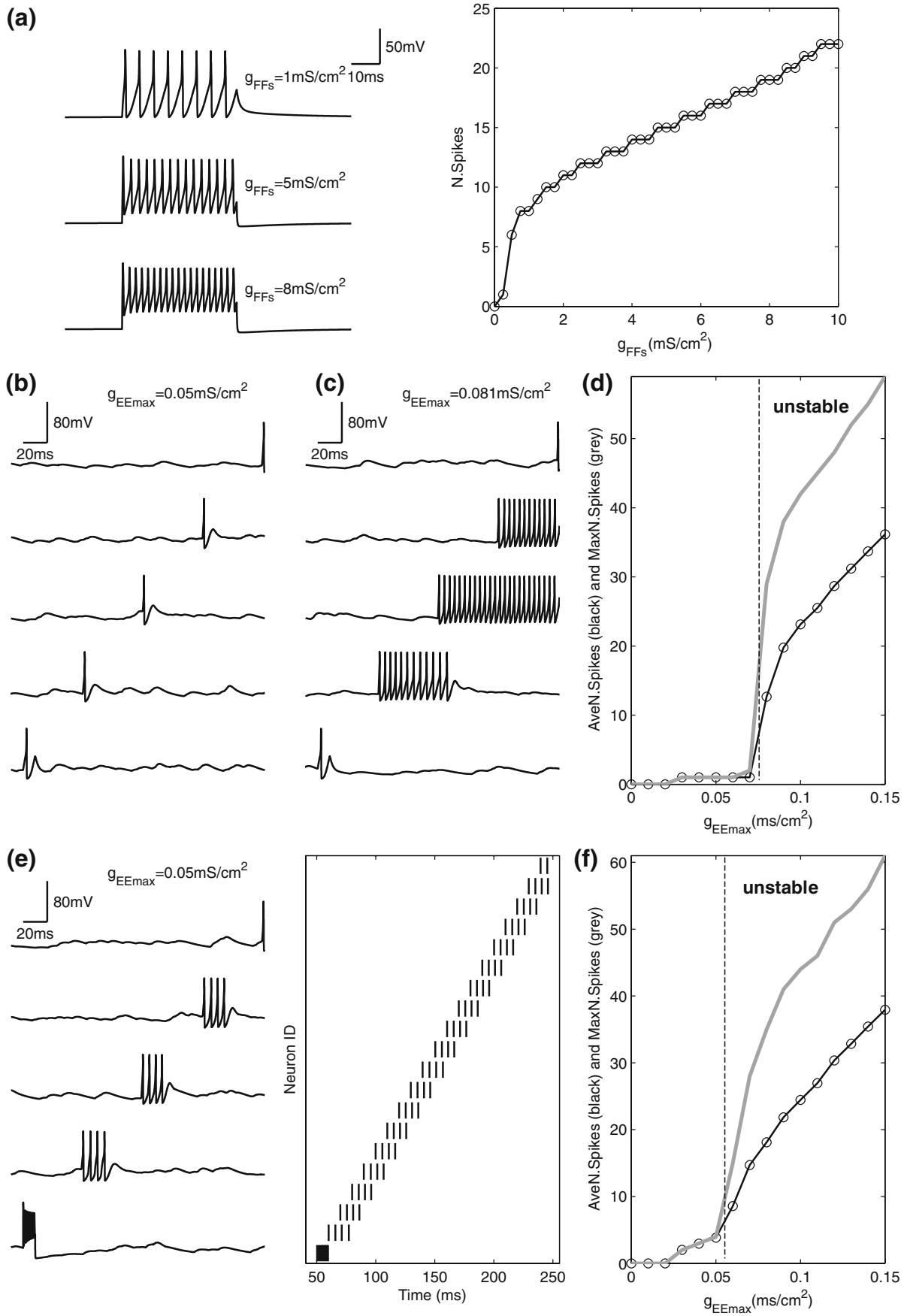
(a)
50mV
10ms
g_{FFs}=1mS/cm^2
g_{FFs}=5mS/cm^2
g_{FFs}=8mS/cm^2
N.Spikes
g_{FFs}(mS/cm^2)
(b)
g_{EEmax}=0.05mS/cm^2
80mV
20ms
(c)
g_{EEmax}=0.081mS/cm^2
80mV
20ms
(d)
unstable
AveN.Spikes (black) and MaxN.Spikes (grey)
g_{EEmax}(ms/cm^2)
(e)
g_{EEmax}=0.05mS/cm^2
80mV
20ms
Neuron ID
Time (ms)
(f)
unstable
AveN.Spikes (black) and MaxN.Spikes (grey)
g_{EEmax}(ms/cm^2)

◀ **Fig. 5** Numerical simulations of sequence generation using model neurons without intrinsic bursting. (**a**) The spiking output of the neuron depends strongly on the amplitude and duration of the input. Constant step excitatory conductance is injected to the neuron. The voltage traces show the response of the neuron to several values of the amplitude g_{FFs} of the injected conductance. The number of spikes versus g_{FFs} is also plotted. (**b**) Voltages of selected neurons in the network versus time. For g_{EEmax}=0.05 mS/cm^2 activity can propagate through the chain, with each neuron spiking exactly once. The neurons of the first group were stimulated to spike once with current injections lasting 10 ms. (**c**) Runaway instability. The condition is the same as in (**b**), except g_{EEmax}=0.081 mS/cm^2. Successive groups produce more spikes. (**d**) Number of spikes per neuron versus g_{EEmax} (*black line and circles*), when single spikes are induced in the first group. Also plotted is the maximum number of spikes in a neuron excluding the first five groups (*grey line*). The divergence between the grey and black lines indicates unstable propagation. (**e**) When each neuron of the first groups was stimulated to spike eight times, burst activity propagated through the chain for g_{EEmax}=0.05 mS/cm^2, with each neuron spiking four time. Spike raster of 20 selected neurons are also shown. (**f**) Number of spikes per neuron versus g_{EEmax} (*black line and circle*) and the maximum number of spikes in a neuron excluding the first five groups (*grey line*), with the same stimulation condition as in (**e**). Runaway excitation occurs when g_{EEmax}>0.07 mS/cm^2

model neuron can fire repeatedly under short current pulses: 10 Hz triangular current pulses with 5 ms rise-time can induce spikes at each pulse (Fig. 4(g)). This is due to a faster rise of the membrane potential compared to the activation of KLT conductance at each pulse, and the reduction of KLT conductance when the membrane potential returns to the resting potential after each pulse. In contrast, triangular pulses with 20 ms rise-time cannot make the neuron spike, as shown in Fig. 4(h).

2.2 Single compartment model

To show how the strong spike-frequency adaptation and the dendritic compartment contribute to robust propagation of burst spikes, we also study spike propagation in networks of the standard Hodgkin–Huxley model with a leak conductance, fast sodium and potassium conductances, and an additional KHT conductance. The properties of the conductances are the same as in the two-compartment model.

2.3 Noise injection

Noisy fluctuation of the membrane potential of each neuron is induced by injection of Poisson spike trains to an excitatory synapse (noise synapse) on the neuron. At each noise spike arrival, the conductance added to the noise synapse is randomly chosen from a range. The parameters of the noise injection are chosen to make the membrane potential to fluctuate with a standard deviation of approximately 3 mV. Specifically, the frequencies and the maximum conductances of the noise spike trains are: 200 Hz and 0.016 mS/cm^2 for the two-compartment model, injected to both the soma and the dendrite; 200 Hz and 0.031 mS/cm^2 for the single compartment models.

2.4 Numerical integration

The dynamical equations are integrated numerically with a fourth-order Runge–Kutta method (Press et al. 1992) using a fixed time step of 0.01 ms. The computer code related to the model is available upon request.

3 Results

3.1 Non-robust burst sequence generation

A complete model of burst sequences in HVC requires not only synaptic connectivity, but also dynamical models of action potential generation and synaptic transmission. In the past, theorists have studied models of sequence generation in which the output of a single neuron is binary-valued (Amari 1972; Kleinfeld 1986), while others have used more realistic spiking neuron models (Abeles 1982, 1991; Cateau and Fukai 2001; Diesmann et al. 1999; Hermann et al. 1995). In our numerical simulations, we have used spiking, conductance-based model neurons. This is because our goal is to identify which intrinsic cellular properties of HVC (RA) neurons are important in the generation of burst sequences.

In the simulations of Fig. 5, we started with model neurons *lacking* intrinsic bursting. These neurons were modified, single compartment, Hodgkin–Huxley models (see Section 2). The properties of the neuron under constant conductance injection are shown in Fig. 5(a). The neuron is regular spiking: it spikes more with larger injected conductance.

The connections between HVC(RA) neurons are thought to be glutamatergic since HVC(RA) neurons are projection neurons that drive RA neurons. In our simulations, the time constants of the synaptic conductances were 5 ms, which is reasonable assuming that the AMPA-subtype of glutamate receptor dominates the NMDA-subtype.

The synaptic strengths were chosen randomly between 0 and a maximal value g_{EEmax}. This value was varied in the different simulations of Fig. 5. Figure 5(b) shows the dynamics for g_{EEmax}=0.05 mS/cm^2. A single spike was stimulated in all neurons of the first group, via current injection lasting 10 ms. Spiking of the first group caused all neurons of the second group to fire a single spike. This excited the third group, and so on down the chain. This type of dynamics has been studied in the synfire chain model (Abeles 1982; Cateau and Fukai 2001; Diesmann et al. 1999; Hermann et al. 1995; Reyes 2003).

Similar behavior was observed for a range of synaptic strengths, g_{EEmax}=0.03 to 0.07 mS/cm^2. Above this range (g_{EEmax}>0.07 mS/cm^2), runaway excitation occurred, as shown in Fig. 5(c). Moving downstream along the chain, each group of neurons spiked for a longer duration than the one before. This type of activity pattern is inconsistent with the bursts observed in HVC, which are of fairly uniform duration. Figure 5(d) shows the dependence of the number of spikes per neuron on g_{EEmax}, averaged over the entire chain, as well as the maximum number of spikes observed in a neuron. In the unstable regime, the maximum number of spikes far exceeds the averaged number of spikes.

It is also possible to obtain propagation of bursts through the network, rather than single spikes. Figure 5(e) shows this phenomenon. To initiate burst propagation, we stimulated eight spikes in neurons of the first group, via current injection lasting 10 ms. Bursting of the first group excited the second group, which excited the third group, and so on. Every burst in the sequence consisted of four spikes. Note that the burst of a group begins before the burst of the previous group ends. Three to four spikes per burst resulted for a small range of synaptic strength, g_{EEmax}=0.04 to 0.05 mS/cm^2. However, this parameter range was also close to a runaway instability, as shown in Fig. 5(f).

Burst sequence generation with neurons lacking intrinsic bursting thus suffers two problems. One is sensitivity to the initial conditions. For a given connection strength, either single spikes or bursts can propagate, depending on how the neurons in the first group are stimulated.[7] The other is that the runaway excitation limits the range of the synaptic strength that can support burst propagation even with the controlled initial conditions.

The model neuron used in these simulations has a high-threshold potassium conductance to enhance its ability to spike at high rates. Even if this conductance is removed, the runaway instability remains. The model neuron has class II spiking behavior (i.e. the minimum frequency of the regular spiking regime is non-zero) (Hodgkin 1948; Rinzel and Ermentrout 1989), but similar results are obtained for neurons with class I spiking behavior (i.e. the neuron can spike regularly at arbitrarily low frequencies).

The problem of runaway instability can be solved in many different ways. Spike frequency adaptation, synaptic depression, or/and recurrent inhibition have all been proposed to stabilize the propagation of spikes through excitatory synaptic connections (Cateau and Fukai 2001; Diesmann et al. 1999; Ermentrout 1998; Golomb and Amitai 1997; Kistler 2000; Kistler and Gerstner 2002; Osan et al. 2004; Traub et al. 1993). In the next section, we propose another solution: intrinsically bursting model neurons. This mechanism also eliminates the sensitivity to the initial conditions.

3.2 Intrinsic bursting

Figure 5(a) depicts the model neuron without intrinsic bursting mechanisms. With the right synaptic input, a burst of several spikes can be stimulated. Note that the number of spikes generated in the burst depends strongly on the amplitude and duration of the input. Therefore it is not surprising that the number of spikes per burst depended sensitively on the synaptic strengths in the network simulations of Fig. 5.

An intrinsically bursting model neuron is shown in Fig. 6. Our model is inspired by previous experimental and modeling results on cortical and hippocampal neurons (Schwindt and Crill 1999; Traub et al. 1994; Wong and Stewart 1992). Both somatic and dendritic voltages are modeled, along with dendritic calcium concentration. If synaptic input to the dendrite exceeds a threshold, a dendritic spike is initiated. The dendritic spike is caused by positive feedback between voltage and voltage-gated calcium channels, so it is also appropriate to use the term "calcium spike."

A calcium spike in the dendrite sends current into the soma, producing sodium spikes. Because calcium dynamics is relatively slow, the calcium spike has a longer duration than a typical sodium spike. Therefore, a burst of several spikes is produced.

Here the most significant point is the stereotypy of the somatic response to a dendritic spike, as shown in Fig. 6(a). If the synaptic input is below the threshold for generation of a dendritic spike, it is not strong enough to initiate a somatic spike. If the synaptic input is suprathreshold, varying its amplitude and duration causes little change in the somatic spiking pattern.[8] The reason is that most of the current driving somatic spiking comes from the calcium spike; the synaptic current has little direct effect. Furthermore, the calcium spike is a stereotyped event, because it is caused by active dendritic processes.

Because of the stereotypy of the burst of somatic spikes, it is plausible that a network composed of intrinsically bursting neurons can produce HVC-like activity with little

[7] If the connection strength supports a stable propagation of single spikes, it is possible to propagate any number of spikes per neuron by inducing long spike trains at low frequency in the neurons of the first group (data not shown). Such propagation however does not agree with the observed short high frequency (about 600 Hz) bursts of spikes in HVC(RA) neurons (Hahnloser et al. 2002).

[8] The number of spikes decreases slightly with the increase of the synaptic input to the dendrite (Fig. 6(a)). This is because the reversal potential of the calcium current (120 mV) is much larger than that of the synaptic current (0 mV). Increasing the synaptic input thus slightly decreases the strength of the calcium spike.

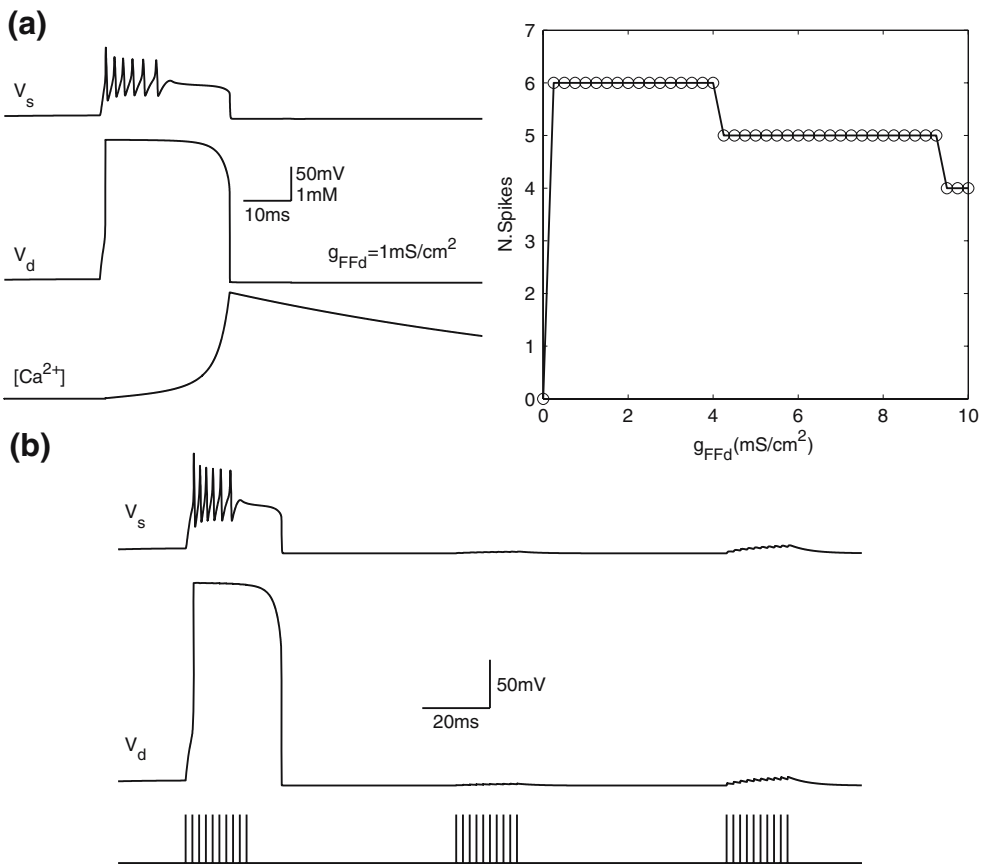

Fig. 6 The dendritic mechanism of burst generation in the two-compartment model of HVC(RA) neuron. (**a**) The spiking output of the neuron depends only weakly on the amplitude g_{FFd} and duration of constant excitatory conductance input on the dendrite. Somatic voltage, dendritic voltage, and dendritic calcium concentration are shown. Input conductance to the dendrite causes a dendritic spike, which drives a burst of somatic spikes. (**b**) The dendritic spike has a long refractory period. Only the first synaptic input in a series of three is able to activate a dendritic spike. The vertical bars indicate the times of excitatory synaptic inputs to the dendrite

need for fine tuning. This will be demonstrated in the next section.

Another important feature of the dendritic spike is its long refractory period. In Fig. 6(b), the dendrite receives three identical synaptic inputs, spaced by 80 ms intervals. Although the first input causes a dendritic spike, the second and third fail to do so. This is because calcium concentration decays slowly after the dendritic spike, and activates a calcium-dependent potassium current, which reduces the excitability of the dendrite. As will be seen in the next section, the long refractory period also contributes to prevention of runaway instability.

It should be noted that there is presently no published evidence for dendritic calcium spikes in HVC(RA) neurons. We *predict* that this phenomenon will be found (see Section 4).

3.3 Robust burst sequence generation

We simulated a network of intrinsically bursting model neurons, with the synaptic connectivity of Fig. 3(b). Some simulated burst sequences are shown in Fig. 7(a). Each burst of somatic spikes rides on top of a "plateau" in voltage. The plateau is due to current generated by the dendritic spike. In effect, dendrites use somatic spikes to communicate with each other. If we considered only somatic spike times, the activity of this model would look very similar to the activity shown in Fig. 5. However, the model is very different, because the fundamental propagating event is the dendritic spike, not the somatic spike.

Intrinsic bursting gives the model improved robustness. If g_{EEmax} is varied, the number of spikes per burst varies from 4 to 6 (Fig. 7(c)). As explained before, this is because a burst is a stereotyped event. Furthermore, there is no runaway instability. The stereotypy of the calcium spike makes the neural response insensitive to the synaptic inputs. This prevents amplification of the activity during the propagation. The long refractory period of the dendritic spike also contributes to the stability by suppressing consecutive activations of the dendrtic spikes.

3.4 Strong spike frequency adaptation

Our model neuron has another important feature, which is that the burst of somatic spikes has a shorter duration than the calcium spike (see Fig. 6(a)). The somatic spikes terminate because the soma has a low threshold potassium (KLT) conductance, which strongly dampens excitability when the soma is depolarized.

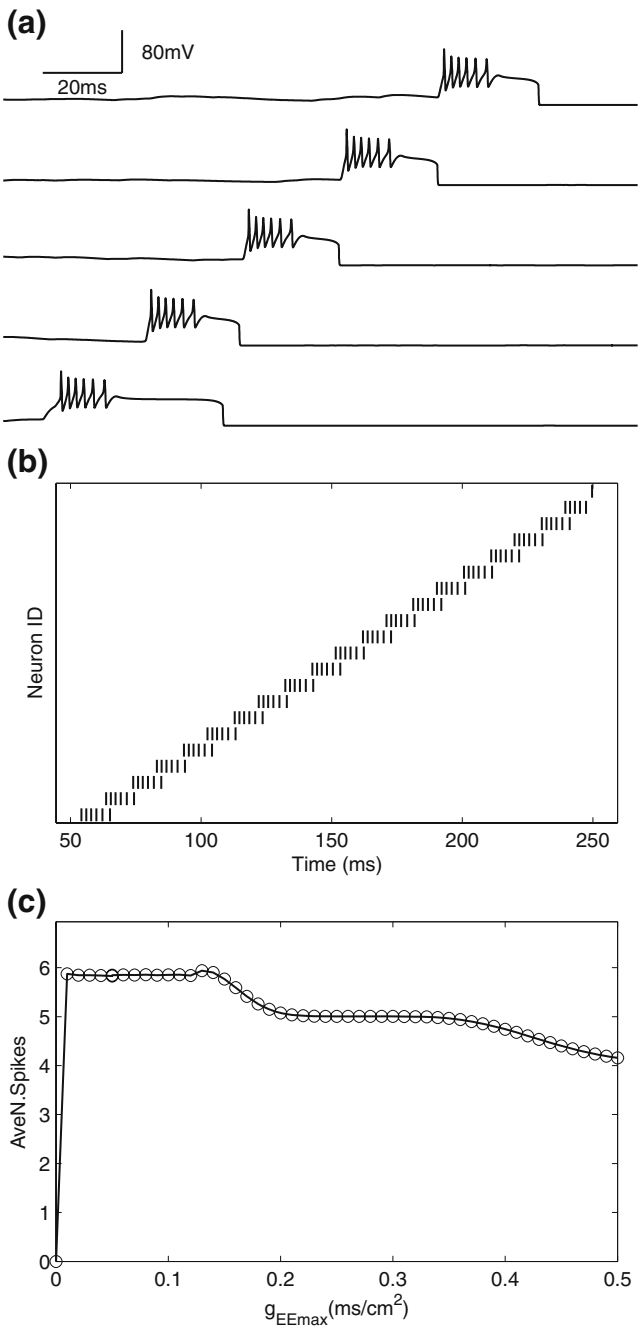

Fig. 7 Robust propagation of burst spikes in networks of the HVC (RA) neurons with active dendrites. (**a**) Traces of somatic membrane potentials of five selected neurons in a run of the dynamics. The connections between the neurons are made to the dendrites. (**b**) Spike raster of 20 selected neurons. (**c**) Average number of spikes per neuron versus the connection strength g_{EEmax}

Our use of a KLT conductance is inspired by Dutar et al. (1998), who used sharp electrodes to record from HVC (RA) neurons in brain slices from adult zebra finches. They found that HVC(RA) neurons responded with just one or two spikes to sustained current injection. They also noted that the strong spike frequency adaptation might be due to a rapidly activating potassium conductance. Indeed, the KLT conductance has been shown to lead to a similar spike response in a number of other neuron types, including auditory neurons in avian nucleus magnocellularis (Rathouz and Trussell 1998; Reyes et al. 1994), bushy cells in ventral cochlear nucleus (Manis and Marx 1991), auditory neurons in medial nucleus of the trapezoid body of rats (Dodson et al. 2002) and mice (Wang et al. 1998), and auditory neuron in gerbil medial superior olive (Svirskis et al. 2002).

Whether a KLT conductance is likewise the mechanism of spike frequency adaptation in HVC(RA) neurons is presently unknown. Our model cannot resolve this issue; further experiments are needed. The point of our model is different: it proposes a possible *function* for spike frequency adaptation, regardless of its biophysical mechanism. Adaptation allows the duration of somatic spiking to be shorter than the duration of the dendritic calcium spike. This is an important feature, since the typical burst of sodium spikes in HVC(RA) neurons during singing is just 6 ms (Hahnloser et al. 2002), whereas the dendritic calcium can last tens of milliseconds if the hypothetical calcium spikes in dendrities of HVC(RA) neurons are similar to calcium spikes in cortical and hippocampal neurons. In our model, the short burst duration is set by the properties of the KLT conductance.

3.5 Robustness of intrinsic bursting

If the neurons are intrinsically bursting, the need for fine-tuning of synaptic strengths is removed from our model. However, one might ask whether fine-tuning of intrinsic cellular properties is necessary to achieve the proper burst duration and number of spikes per burst. To investigate this issue, we experimented with varying parameters of the model dendrite. Figure 8 shows the effect of these manipulations on the number of spikes per burst.

Figure 8(a) shows how the spike number depends on the coupling resistance R_c between the dendritic and somatic compartments, and the total dendritic area A_d. All other parameters are left at their default values. The spike number is insensitive to A_d. The dependence on R_c is stronger, but there is a reasonable range of values yielding more than three spikes.

Figure 8(b) plots the dependence of the number of somatic spikes on the conductances g_{Ca} and g_{CaK} of calcium channels and calcium-activated potassium channels, respectively. There is a large parameter regime in which the spike number is 5 or 6.

The problem of how excitable cells regulate their conductances to achieve dynamical behaviors is a fascinating one. The problem is not peculiar to our model of HVC,

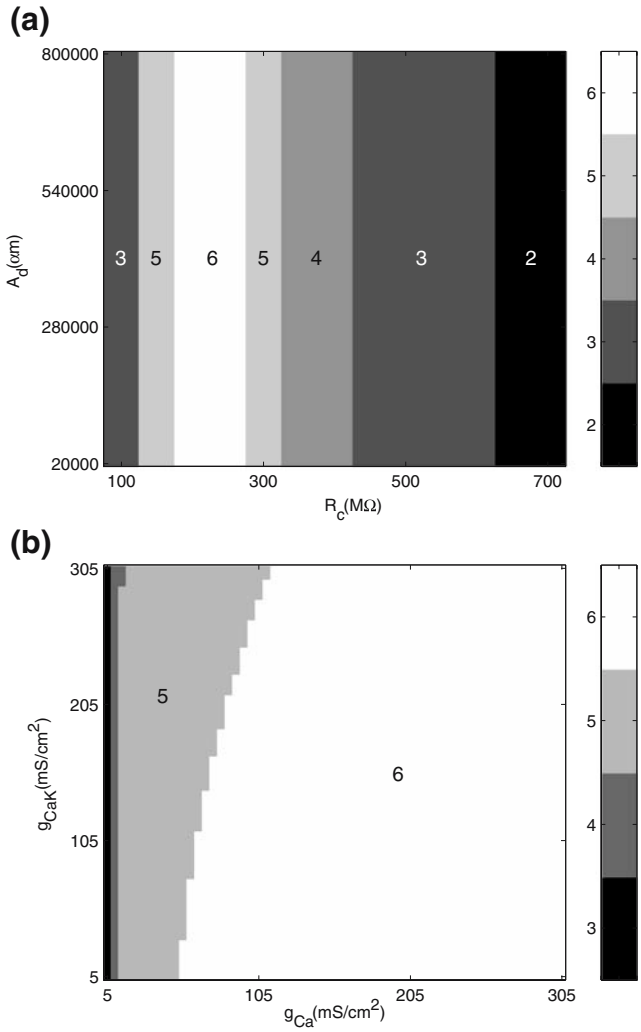

Fig. 8 Robustness of intrinsic bursting to changes in parameters of the HVC(RA) neuron model. (**a**) Dependence of spike number on soma-dendrite coupling and total dendritic area. (**b**) Dependence of spike number on conductances of calcium channels and calcium-activated potassium channels

but is relevant to just about any neural system. It seems likely that such regulatory mechanisms exist (Davis 2006). Figure 8 suggests that such mechanisms would not have to tune parameters very precisely to achieve the required bursting behavior.

4 Discussion

In conclusion, we have described a theory of burst sequences in HVC(RA) neurons that is based on two main hypotheses. Hypothesis 1 is that the connectivity between HVC(RA) neurons is correlational, i.e., based on temporal correlations in their activity. Hypothesis 2 is that HVC(RA) neurons are intrinsic bursters.

4.1 Correlational connectivity

Hypothesis 1 makes a clear prediction: two HVC(RA) neurons that burst in succession should be connected by an excitatory synapse, with high probability. While this hypothesis is easy to state, the only direct experimental tests that one can imagine are very difficult. For example, one could perform dual intracellular recordings of pairs of HVC(RA) neurons in singing birds. One could test whether the neurons are connected, and then compare their burst timings. To a neurophysiologist, this experiment already sounds extremely difficult. To make things worse, connections between HVC(RA) neurons are likely to be very sparse. In our numerical simulations, we used 200 groups of neurons. If a pair of neurons is chosen randomly from our model, its probability of being connected is less than 1%. Therefore, our model predicts that it would be difficult to find connected pairs by simply recording randomly from neurons.[9]

If HVC were spatially organized, the experimental situation would be more favorable. For example, suppose that neurons that burst simultaneously were at the same location in HVC. Then it would be much easier to find connected pairs of neurons. However, no such spatial organization has been detected so far (Fee, unpublished observations).

An alternative to the neurophysiological approach mentioned above is a purely anatomical approach. Recently, new high-throughput anatomical techniques have been invented (Denk and Horstmann 2004; Tsai et al. 2003). In particular, automated serial-section electron microscopy could potentially allow the reconstruction of the entire synaptic connectivity of HVC. If HVC were found to have a connectivity similar to one of those shown in Fig. 3, this would be strong evidence for Hypothesis 1.

To some, Hypothesis 1 may seem so intuitively obvious that its truth must be a foregone conclusion. But this is not the case, as competing models for sequence generation have been proposed. For example, Estes argued that sequential order is determined by inhibitory synaptic connectivity, not excitatory connectivity (Estes 1972).

4.2 Intrinsic bursting

We have shown that intrinsic bursting enhances the robustness of burst sequence generation by a neural network. According to our Hypothesis 2, HVC(RA) neurons are intrinsic bursters. How strong is this prediction? It is consistent with the observation that the spontaneous bursts of HVC(RA) neuron during sleep have the same stereotypy as during singing

[9]While Mooney and Prather reported synaptic interactions between pairs of HVC(RA) neurons in vitro (Mooney and Prather 2005), it is not clear whether these connections were monosynaptic.

(Hahnloser et al. 2002, 2006). While intrinsic bursting is one solution to the problem of robustness, it is not the only one. Other biophysical mechanisms could also improve robustness, such as spike frequency adaptation, synaptic depression, and recurrent inhibition (Cateau and Fukai 2001; Diesmann et al. 1999; Ermentrout 1998; Golomb and Amitai 1997; Kistler 2000; Kistler and Gerstner 2002; Osan et al. 2004; Traub et al. 1993). While our theoretical arguments are suggestive, they are not conclusive. Ultimately, this issue can only be settled by experiment.

In previous experiments in vitro, it has been found that somatic current injection does not trigger intrinsic bursting in HVC(RA) neurons (Dutar et al. 1998; Kubota and Taniguchi 1998; Mooney 2000; Wild et al. 2005). This may sound inconsistent with our Hypothesis 2, but actually it is not, for two reasons. First, somatic current injection is an indirect way of testing for a dendritic spike. In our model, it may or may not trigger a calcium spike in the dendrite. This depends on model parameters like the strength of coupling between the soma and dendrite, and the voltage threshold for a dendritic spike. Second, the intrinsic properties of HVC(RA) neurons appear to be different in vitro and in the brain of a singing bird. For example, the peak firing rates observed in vitro are never as high as those observed during song (Dutar et al. 1998; Kubota and Taniguchi 1998). Perhaps HVC(RA) neurons in vitro are missing some neuromodulator that is necessary for the intrinsic properties appropriate for song-related activity, and this neuromodulator could have effects on intrinsic bursting.

Given these facts, one can imagine a number of ways of testing Hypothesis 2. Drugs that affect voltage-gated calcium channels or calcium-activated potassium channels could lower the threshold for a dendritic spike, and permit the initiation of a burst by somatic current injection. Furthermore, such drugs could change burst duration or spike number during song *in vivo*. In addition, glutamate uncaging could be used to stimulate dendrites directly, as has been done with cortical neurons (Schiller et al. 2000; Wei et al. 2001). Also *in vivo* imaging of calcium dynamics in dendrites could be revealing (Euler et al. 2002; Trachtenberg et al. 2002).

4.3 Spike frequency adaptation

We have argued that strong spike frequency adaptation in HVC(RA) neurons could function to make burst duration shorter than the duration of the hypothetical dendritic calcium spike. However, we should make the caveat that there is some disagreement about the strength of spike frequency adaptation in HVC(RA) neurons. Kubota and Taniguchi (1998) found weaker spike frequency adaptation in HVC(RA) neurons, which in their experiments produced many spikes in response to sustained current injection. Perhaps their results were different from Dutar et al. (1998) because they used patch electrodes rather than sharp electrodes and juvenile rather than adult birds.

Therefore we should also consider the alternative scenario in which spike frequency adaptation is only a weak effect, and has little effect on burst duration. In this scenario, the dendritic calcium spike itself has short duration, unlike calcium spikes seen in cortical and hippocampal neurons (Golding et al. 1999; Schwindt and Crill 1999; Wei et al. 2001).

In short, two scenarios should be considered: burst duration could be set by the time course of the dendritic spike, or by somatic spike frequency adaptation. These possibilities can be tested pharmacologically by applying drugs that affect calcium dynamics or spike frequency adaptation and observing the effects on burst duration during song.

4.4 Refractory period

In our model, the dendritic spike has a long refractory period, due to the slow decay of calcium and the calcium-dependent potassium current (Fig. 5(b)). Previously we argued that the refractory period could function to prevent runaway instability.

Here we mention another possible effect: the refractory period could enhance robustness to sloppiness in the connectivity of the HVC(RA) neurons. In our idealized model, if neuron A bursts *after* neuron B, there is no synaptic connection from A to B. In Fig. 3, this dependence on temporal order is reflected in the fact that there are only "forward" connections, and no "backward" connections. However, even if there were some backward connections, they would have no effect on propagation of bursts through the network, because they would deliver synaptic input to neurons only while their dendrites are refractory. Therefore, some sloppiness in the connectivity can be tolerated.

Note that burst propagation would be possible in the models of Fig. 3, even if the connectivity were truly bidirectional, with equal numbers of forward and backward connections. Then propagation in either direction would be possible, so that the bird could sing its song either forward or backward.[10] Since this is not observed, it seems more likely that the connectivity is biased in the forward direction.

4.5 Inhibition

In our model, we neglected the influence of HVC(I) neurons on HVC(RA) neurons. We argued that this was a

[10]Bidirectional propagation is standard for most *excitable media*. For example, an axon can support either orthodromic or antidromic propagation of an action potential, though only the orthodromic is seen in natural conditions.

good approximation because the spiking of HVC(I) neurons is much less temporally selective, and therefore their input to HVC(RA) neurons can be approximated as constant in time. We suspect that interneurons lack temporal selectivity because they sum the outputs of many projection neurons. Because the projection neurons are active at a wide variety of times, the sum of their outputs is temporally unselective.

While inhibition is not expected to determine the temporal order in which projection neurons are activated, it may have the function of regulating the overall level of activity of the projection neurons. In other words, inhibition could be a circuit mechanism that prevents runaway instability, in addition to the cellular mechanisms that have been discussed previously.

4.6 Learning

Suppose that HVC(RA) neurons possess a correlational connectivity, like those of Fig. 3. How could this connectivity be created during learning or development?

The simplest possibility would be spatial organization. Suppose that the HVC(RA) neurons were arranged so that their temporal selectivities progressed in an orderly fashion across HVC. Then if synaptic connections were local in space and biased in one direction, they would conform to Fig. 3. However, as mentioned previously, no such spatial organization has been detected in HVC(RA) neurons thus far.

The obvious alternative is that Hebbian synaptic plasticity could create correlational structure. This idea has been popular in models of associative memory, in which synaptic strengths are given by correlation matrices. The idea was proposed for temporal sequences in particular by Amari (1972).

4.7 Previous models of HVC sequence generation

In a previous model of sequence generation by HVC, Troyer and Doupe proposed that sequences are generated by an associative chain of motor and sensory representations (Troyer and Doupe 2000), where the motor representation resides in the HVC(RA) neurons and the sensory representation is an efference copy in the HVC(X) neurons. The sequence is generated by reciprocal excitatory interactions between the HVC(RA) and HVC(X) neural populations. In contrast, we have argued that the associative chain is within the HVC(RA) population itself, and does not involve the HVC(X) neurons. Support for this idea comes from the fact that targeted destruction of HVC(X) neurons does not cause deterioration of song in adult zebra finches (Scharff et al. 2000). Accordingly, we believe that there are excitatory synapses from HVC(RA) to HVC(X) neurons, but not vice versa (see Fig. 2).

Drew and Abbott proposed a model of sequence generation in HVC (Drew and Abbott 2003). In the model, HVC neurons are driven with a common periodic input. The sequential firing of the neurons arise from chained inhibitory connections between neurons, disinhibition, as well as strong afterhyperpolarization currents that prevent neurons to spike repeatedly in short time. Their work is closely related to the general model of sequence generation proposed by Estes (1972). Although there is some evidence of sporadic timed inputs from Uva (Vu et al. 1994; Williams and Vicario 1993), it has not been demonstrated that there are timing signals with high enough resolution to drive sequential burst of spiking lasting about 6 ms. Our model does not require a timing signal inputs. The timing arises from the excitatory connectivity between the neurons. However our model does require an external input to start the spiking activity in the first group.

In their model of birdsong learning, Doya and Sejnowski (1999) took the HVC activation patterns as given. They did not address the mechanism of sequence generation in HVC.

4.8 Synfire chains

Spiking network models utilizing the connectivity of Fig. 3(b) are often called *synfire chains*. Should this term also be applied to the present model? The answer to this question depends on the exact definition of the term. Typically *synchronous spiking* of one group of neurons is required to drive the next group over threshold in a synfire chain. Having a high threshold for spiking helps to make the dynamics robust to noise. Also, each neuron in a group generates a single spike, so that the precise timing of this spike is clearly important. On the other hand, suppose that each neuron generates a burst of more than one spike, and synapses must temporally integrate successive spikes to drive the next group of neurons above threshold. In this case, the spiking of neurons in a group must still occur within a window that is set by the synaptic integration time. However, the width of this window is longer than the interspike interval during a burst, so it is not clear whether this qualifies as precise synchrony.

In our model of burst sequences, the dendritic calcium spike is the fundamental propagating event, rather than the somatic sodium spikes. Therefore, the term *synburst* chain might be more appropriate.[11]

[11] Another ambiguity of definition arises when considering the connectivity of Fig. 3(c). In this model, the connectivity is unidirectional but the neurons are not divided into groups. Here the spike times of the neurons will not cluster into groups, but are expected to be fairly uniformly distributed in time. Nevertheless, synchronous (within a synaptic integration time) spiking may be required for propagation of activity. It is not clear whether this should be called a *synfire chain*.

Acknowledgement Research was supported by The Huck Institute of Life Sciences at the Pennsylvania State University and Alfred P. Sloan Fellowship (DZJ), and Howard Hughes Medical Institute (FR, HSS). DZJ thanks the Kavli Institute for Theoretical Physics at University of California, Santa Barbara for partial support of this work. We thank Michael Long, Anthony Leonardo and Michale Fee for useful discussions.

References

Abeles, M. (1982). *Local cortical circuits: An electrophysiological study* (pp. 83–92). Berlin Heidelberg New York: Springer.

Abeles, M. (1991). *Corticonics*. Cambridge, UK: Cambridge University Press.

Amari, S. (1972). Learning patterns and pattern sequences by self-organizing nets of threshold elements. *IEEE Transactions on Computers*, *C-21*, 1197–1206.

Brainard, M. S., & Doupe, A. J. (2000). Interruption of a basal ganglia-forebrain circuit prevents plasticity of learned vocalizations. *Nature*, *404*, 762–766.

Brumberg, J. C., Nowak, L. G., & McCormick, D. A. (2000). Ionic mechanisms underlying repetitive high-frequency burst firing in supragranular cortical neurons. *Journal of Neuroscience*, *20*, 4829–4843.

Cardin, J. A., Raksin, J. N., & Schmidt, M. F. (2004). The sensorimotor nucleus NIf is necessary for auditory processing but not vocal motor output in the avian song system. *Journal of Neurophysiology.*

Cateau, H., & Fukai, T. (2001). Fokker–Planck approach to the pulse packet propagation in synfire chain. *Neural Networks*, *14*, 675–685.

Chi, Z., & Margoliash, D. (2001). Temporal precision and temporal drift in brain and behavior of zebra finch song. *Neuron*, *32*, 899–910.

Coleman, M. J., & Vu, E. T. (2005). Recovery of impaired songs following unilateral but not bilateral lesions of nucleus uvaeformis of adult zebra finches. *Journal of Neurobiology*, *63*, 70–89.

Crook, S. M., Ermentrout, G. B., & Bower, J. M. (1998). Spike frequency adaptation affects the synchronization properties of networks of cortical oscillations. *Neural Computation*, *10*, 837–854.

Davis, G. W. (2006). Homeostatic control of neural activity: From phenomenology to molecular design. *Annual Review of Neuroscience*, *29*, 307–323.

Denk, W., & Horstmann, H. (2004). Serial block-face scanning electron microscopy to reconstruct three-dimensional tissue nanostructure. *PLoS Biol*, *2*, e329.

Diesmann, M., Gewaltig, M. O., & Aertsen, A. (1999). Stable propagation of synchronous spiking in cortical neural networks. *Nature*, *402*, 529–533.

Dodson, P. D., Barker, M. C., & Forsythe, I. D. (2002). Two heteromeric Kv1 potassium channels differentially regulate action potential firing. *Journal of Neuroscience*, *22*, 6953–6961.

Doupe, A. J., & Kuhl, P. K. (1999). Birdsong and human speech: Common themes and mechanisms. *Annual Review of Neuroscience*, *22*, 567–631.

Doya, K., & Sejnowski, T. J. (1999). A computational model of avian song learning. In M. S. Gazzaniga (Ed.), *The new cognitive neurosciences*. Cambridge, MA: MIT Press.

Drew, P. J., & Abbott, L. F. (2003). Model of song selectivity and sequence generation in area HVc of the songbird. *Journal of Neurophysiology*, *89*, 2697–2706.

Dutar, P., Vu, H. M., & Perkel, D. J. (1998). Multiple cell types distinguished by physiological, pharmacological, and anatomic properties in nucleus HVc of the adult zebra finch. *Journal of Neurophysiology*, *80*, 1828–1838.

Ermentrout, B. (1998). The analysis of synaptically generated traveling waves. *Journal of Computational Neuroscience*, *5*, 191–208.

Estes, W. K. (1972). An associative basis for coding and organisation in memory. In A. W. Melton, & E. Martin (Eds.), *Coding processes in human memory*. Washington, DC: Winston.

Euler, T., Detwiler, P. B., & Denk, W. (2002). Directionally selective calcium signals in dendrites of starburst amacrine cells. *Nature*, *418*, 845–852.

Fee, M. S., Kozhevnikov, A. A., & Hahnloser, R. H. (2004). Neural mechanisms of vocal sequence generation in the songbird. *Annals of the New York Academy of Sciences*, *1016*, 153–170.

Fortune, E. S., & Margoliash, D. (1995). Parallel pathways and convergence onto HVc and adjacent neostriatum of adult zebra finches (*Taeniopygia guttata*). *Journal of Comparative Neurology*, *360*, 413–441.

Franceschetti, S., Guatteo, E., Panzica, F., Sancini, G., Wanke, E., & Avanzini, G. (1995). Ionic mechanisms underlying burst firing in pyramidal neurons: Intracellular study in rat sensorimotor cortex. *Brain Research*, *696*, 127–139.

Golding, N. L., Jung, H. Y., Mickus, T., & Spruston, N. (1999). Dendritic calcium spike initiation and repolarization are controlled by distinct potassium channel subtypes in CA1 pyramidal neurons. *Journal of Neuroscience*, *19*, 8789–8798.

Golomb, D., & Amitai, Y. (1997). Propagating neuronal discharges in neocortical slices: Computational and experimental study. *Journal of Neurophysiology*, *78*, 1199–1211.

Hahnloser, R. H., Kozhevnikov, A. A., & Fee, M. S. (2002). An ultra-sparse code underlies the generation of neural sequences in a songbird. *Nature*, *419*, 65–70.

Hahnloser, R. H., Kozhevnikov, A. A., & Fee, M. S. (2006). Sleep-related neural activity in a premotor and a basal-ganglia pathway of the songbird. *Journal of Neurophysiology*, *96*, 794–812.

Hausser, M., Spruston, N., & Stuart, G. J. (2000). Diversity and dynamics of dendritic signaling. *Science*, *290*, 739–744.

Hermann, M., Hertz, J. A., & Prugel-Bennet, A. (1995). Analysis of synfire chains. *Network: Computation in Neural Systems*, *6*, 403–414.

Hodgkin, A. L. (1948). The local electric changes associated with repetitive action in a non-medulated axon. *Journal of Physiology*, *107*, 165–181.

Hodgkin, A. L., & Huxley, A. F. (1952). A quantitative description of membrane current and its application to conduction and excitation in nerve. *Journal of Physiology (London)*, *117*, 500–544.

Immelmann, K. (1969). Song development in the zebra finch and other estrildid finches. In R. Hinde (Ed.), *Bird vocalization* (pp. 61–74). Cambridge, UK: Cambridge University Press.

Katz, L. C., & Gurney, M. E. (1981). Auditory responses in the zebra finch's motor system for song. *Brain Research*, *221*, 192–197.

Kistler, W. M. (2000). Stability properties of solitary waves and periodic wave trains in a two-dimensional network of spiking neurons. *Physical Review. E, Statistical Physics, Plasmas, Fluids, and Related Interdisciplinary Topics*, *62*, 8834–8837.

Kistler, W. M., & Gerstner, W. (2002). Stable propagation of activity pulses in populations of spiking neurons. *Neural Computation*, *14*, 987–997.

Kleinfeld, D. (1986). Sequential state generation by model neural networks. *Proceedings of the National Academy of Sciences of the United States of America*, *83*, 9469–9473.

Konishi, M. (1965). The role of auditory feedback in the control of vocalization in the white-crowned sparrow. *Zeitschrift für Tierpsychologie*, *22*, 770–783.

Kozhevnikov, A., & Fee, M. S. (2006). Singing-related activity of identified HVC neurons in the zebra finch. *Journal of Neurophysiology.*

Kubota, M., & Taniguchi, I. (1998). Electrophysiological characteristics of classes of neuron in the HVc of the zebra finch. *Journal of Neurophysiology*, *80*, 914–923.

Lashley, K. S. (1951). The problem of serial order in behavior. In L. A. Jeffress (Ed.), *Cerebral mechanisms in behavior (the Hixon Symposium)* (pp. 112–136). New York: Wiley.

Leonardo, A., & Fee, M. S. (2005). Ensemble coding of vocal control in birdsong. *Journal of Neuroscience*, *25*, 652–661.

Lewicki, M. S. (1996). Intracellular characterization of song-specific neurons in the zebra finch auditory forebrain. *Journal of Neuroscience*, *16*, 5855–5863.

Lien, C. C., & Jonas, P. (2003). Kv3 potassium conductance is necessary and kinetically optimized for high-frequency action potential generation in hippocampal interneurons. *Journal of Neuroscience*, *23*, 2058–2068.

Manis, P. B., & Marx, S. O. (1991). Outward currents in isolated ventral cochlear nucleus neurons. *Journal of Neuroscience*, *11*, 2865–2880.

Mattia, D., Kawasaki, H., & Avoli, M. (1997). In vitro electrophysiology of rat subicular bursting neurons. *Hippocampus*, *7*, 48–57.

Mooney, R. (2000). Different subthreshold mechanisms underlie song selectivity in identified HVc neurons of the zebra finch. *Journal of Neuroscience*, *20*, 5420–5436.

Mooney, R., Hoese, W., & Nowicki, S. (2001). Auditory representation of the vocal repertoire in a songbird with multiple song types. *Proceedings of the National Academy of Sciences of the United States of America*, *98*, 12778–12783.

Mooney, R., & Prather, J. F. (2005). The HVC microcircuit: The synaptic basis for interactions between song motor and vocal plasticity pathways. *Journal of Neuroscience*, *25*, 1952–1964.

Nixdorf, B. E., Davis, S. S., & DeVoogd, T. J. (1989). Morphology of Golgi-impregnated neurons in hyperstriatum ventralis, pars caudalis in adult male and female canaries. *Journal of Comparative Neurology*, *284*, 337–349.

Nottebohm, F., Kelley, D. B., & Paton, J. A. (1982). Connections of vocal control nuclei in the canary telencephalon. *Journal of Comparative Neurology*, *207*, 344–357.

Nottebohm, F., Stokes, T. M., & Leonard, C. M. (1976). Central control of song in the canary, Serinus canarius. *Journal of Comparative Neurology*, *165*, 457–486.

Osan, R., Curtu, R., Rubin, J., & Ermentrout, B. (2004). Multiple-spike waves in a one-dimensional integrate-and-fire neural network. *Journal of Mathematical Biology*, *48*, 243–274.

Pinsky, P. F., & Rinzel, J. (1994). Intrinsic and network rhythmogenesis in a reduced Traub model for CA3 neurons. *Journal of Computational Neuroscience*, *1*, 39–60.

Press, W., Teukolsky, S., Vetterling, W., & Flannery, B. (1992). *Numerical recipes in C*. Cambridge, UK: Cambridge University Press.

Rathouz, M., & Trussell, L. (1998). Characterization of outward currents in neurons of the avian nucleus magnocellularis. *Journal of Neurophysiology*, *80*, 2824–2835.

Reyes, A. D. (2003). Synchrony-dependent propagation of firing rate in iteratively constructed networks in vitro. *Nature Neuroscience*, *6*, 593–599.

Reyes, A. D., Rubel, E. W., & Spain, W. J. (1994). Membrane properties underlying the firing of neurons in the avian cochlear nucleus. *Journal of Neuroscience*, *14*, 5352–5364.

Rinzel, J., & Ermentrout, G. B. (1989). Analysis of neural excitability and oscillations. In C. Koch, & I. Segev (Eds.), *Methods in neuronal modeling*. Cambridge: MIT Press.

Scharff, C., Kirn, J. R., Grossman, M., Macklis, J. D., & Nottebohm, F. (2000). Targeted neuronal death affects neuronal replacement and vocal behavior in adult songbirds. *Neuron*, *25*, 481–492.

Schiller, J., Major, G., Koester, H. J., & Schiller, Y. (2000). NMDA spikes in basal dendrites of cortical pyramidal neurons. *Nature*, *404*, 285–289.

Schwindt, P., & Crill, W. (1999). Mechanisms underlying burst and regular spiking evoked by dendritic depolarization in layer 5 cortical pyramidal neurons. *Journal of Neurophysiology*, *81*, 1341–1354.

Sompolinsky, H., & Kanter, I. I. (1986). Temporal association in asymmetric neural networks. *Physical Review Letters*, *57*, 2861–2864.

Svirskis, G., Kotak, V., Sanes, D. H., & Rinzel, J. (2002). Enhancement of signal-to-noise ratio and phase locking for small inputs by a low-threshold outward current in auditory neurons. *Journal of Neuroscience*, *22*, 11019–11025.

Trachtenberg, J. T., Chen, B. E., Knott, G. W., Feng, G., Sanes, J. R., Welker, E., et al. (2002). Long-term in vivo imaging of experience-dependent synaptic plasticity in adult cortex. *Nature*, *420*, 788–794.

Traub, R. D., Jefferys, J. G., & Miles, R. (1993). Analysis of the propagation of disinhibition-induced after-discharges along the guinea-pig hippocampal slice in vitro. *Journal of Physiology*, *472*, 267–287.

Traub, R. D., Jefferys, J. G., Miles, R., Whittington, M. A., & Toth, K. (1994). A branching dendritic model of a rodent CA3 pyramidal neurone. *Journal of Physiology*, *481*(Pt 1), 79–95.

Troyer, T. W., & Doupe, A. J. (2000). An associational model of birdsong sensorimotor learning II. Temporal hierarchies and the learning of song sequence. *Journal of Neurophysiology*, *84*, 1224–1239.

Tsai, P. S., Friedman, B., Ifarraguerri, A. I., Thompson, B. D., Lev-Ram, V., Schaffer, C. B., et al. (2003). All-optical histology using ultrashort laser pulses. *Neuron*, *39*, 27–41.

Vicario, D. S. (1991). Organization of the zebra finch song control system: II. Functional organization of outputs from nucleus Robustus archistriatalis. *Journal of Comparative Neurology*, *309*, 486–494.

Vu, E. T., Mazurek, M. E., & Kuo, Y. C. (1994). Identification of a forebrain motor programming network for the learned song of zebra finches. *Journal of Neuroscience*, *14*, 6924–6934.

Wang, L. Y., Gan, L., Forsythe, I. D., & Kaczmarek, L. K. (1998). Contribution of the Kv3.1 potassium channel to high-frequency firing in mouse auditory neurones. *Journal of Physiology*, *509* (Pt 1), 183–194.

Wang, X. J. (1999). Fast burst firing and short-term synaptic plasticity: A model of neocortical chattering neurons. *Neuroscience*, *89*, 347–362.

Wei, D. S., Mei, Y. A., Bagal, A., Kao, J. P., Thompson, S. M., & Tang, C. M. (2001). Compartmentalized and binary behavior of terminal dendrites in hippocampal pyramidal neurons. *Science*, *293*, 2272–2275.

Wild, J. M., Williams, M. N., Howie, G. J., & Mooney, R. (2005). Calcium-binding proteins define interneurons in HVC of the zebra finch (*Taeniopygia guttata*). *Journal of Comparative Neurology*, *483*, 76–90.

Williams, H. (2004). Birdsong and singing behavior. *Annals of the New York Academy of Sciences*, *1016*, 1–30.

Williams, H., & Vicario, D. S. (1993). Temporal patterning of song production: Participation of nucleus uvaeformis of the thalamus. *Journal of Neurobiology*, *24*, 903–912.

Wong, R. K., & Stewart, M. (1992). Different firing patterns generated in dendrites and somata of CA1 pyramidal neurones in guinea-pig hippocampus. *Journal of Physiology*, *457*, 675–687.

Yu, A. C., & Margoliash, D. (1996). Temporal hierarchical control of singing in birds. *Science*, *273*, 1871–1875.